PROTEINS
STRUCTURE ■ FUNCTION ■ BIOINFORMATICS

Clarifying allosteric control of flap conformations in the 1TW7 crystal structure of HIV-1 protease

Katrina W. Lexa,[1] Kelly L. Damm,[1] Jerome J. Quintero,[2] Jason E. Gestwicki,[3] and Heather A. Carlson[1,2]*

[1] Department of Medicinal Chemistry, University of Michigan, Ann Arbor, Michigan 48109-1065
[2] Biophysics Research Division, University of Michigan, Ann Arbor, Michigan 48109-1055
[3] Life Sciences Institute and Department of Pathology, University of Michigan, Ann Arbor, Michigan 48109-2216

ABSTRACT

The 1TW7 crystal structure of HIV-1 protease shows the flaps placed wider and more open than what is seen in other examples of the semi-open, apo form. It has been proposed that this might be experimental evidence of allosteric control, because crystal packing creates contacts to the "elbow region" of the protease, which may cause deformation of the flaps. Recent dynamics simulations have shown that the conformation seen in 1TW7 relaxes into the typical semi-open conformation in the absence of the crystal contacts, definitively showing that the crystal contacts cause the deformation (Layten *et al.*, J Am Chem Soc 2006;128:13360–13361). However, this does not prove or disprove allosteric modulation at the elbow. In this study, we have conducted additional simulations, supplemented with experimental testing, to further probe the possibility of 1TW7 providing an example of allosteric control of the flap region. We show that the contacts are unstable and do not restrict the conformational sampling of the flaps. The deformation seen in the 1TW7 crystal structure is simply opportunistic crystal packing and not allosteric control.

Proteins 2009; 74:872–880.

Key words: molecular dynamics; protein flexibility; drug design; AIDS; ligand binding.

INTRODUCTION

HIV-1 protease (HIVp) inhibitors are essential for current AIDS treatments, and new compounds are still a very active area of research. The conformational behavior of the flap region (residues 43–58) of HIVp has been extensively studied in the last few years, as reviewed by Hornak and Simmerling.[1] X-ray crystallography, NMR spectroscopy, and theoretical studies have established that HIVp may exist in an ensemble of conformations. The most populated states are the closed, semi-open, and open. In the apo form, the thermodynamically favored state is thought to be the semi-open conformation, in which the flaps are loosely positioned over the active site cavity restricting ligand entry.[2–4] A recent coarse-grained dynamics simulation demonstrated that the small cyclic urea inhibitor XK263 can enter the active site from the side when the flaps are semi-open or almost closed.[5] However, the same study also showed that a peptide substrate does not; instead, it samples associating to the surface of the protein until encountering an opening event. It is generally thought that most ligands, particularly the peptide substrate, can only access the active site through the open conformation.[5–7] By restricting flap movement, it may be possible to control binding of the protease substrate to the active site and thereby inhibit activity of HIVp.

Various groups have identified anticorrelated motion between the flap and elbow (residues 35–42) regions through normal mode analysis and molecular dynamics (MD) simulations.[8–11] The closed and semi-open conformations are distinctly different in this region. Restricting movement of the elbow region has been shown to concurrently limit the conformational sampling of the flaps.[12,13] Though only artificial restraints between Cα were used to induce that conformational control, the results demonstrate the elbow region's potential as a site for allosteric regulation that might be manipulated by the binding of a small molecule.

A recent crystal structure of a multidrug-resistant HIVp (1TW7) shows the flaps are wider and more open than in other apo, semi-open structures.[14] Crystal packing creates contacts between the flap tips in the neighboring unit

Additional Supporting Information may be found in the online version of this article.
This work was performed at the University of Michigan, Ann Arbor, MI.
Grant sponsor: National Institutes of Health; Grant numbers: GM65372, GM07767, GM008270.
*Correspondence to: Heather A. Carlson, The University of Michigan, College of Pharmacy, 428 Church St., Ann Arbor, MI 48109-1065. E-mail: carlsonh@umich.edu
Received 8 January 2008; Revised 10 June 2008; Accepted 17 June 2008
Published online 14 August 2008 in Wiley InterScience (www.interscience.wiley.com). DOI: 10.1002/prot.22195

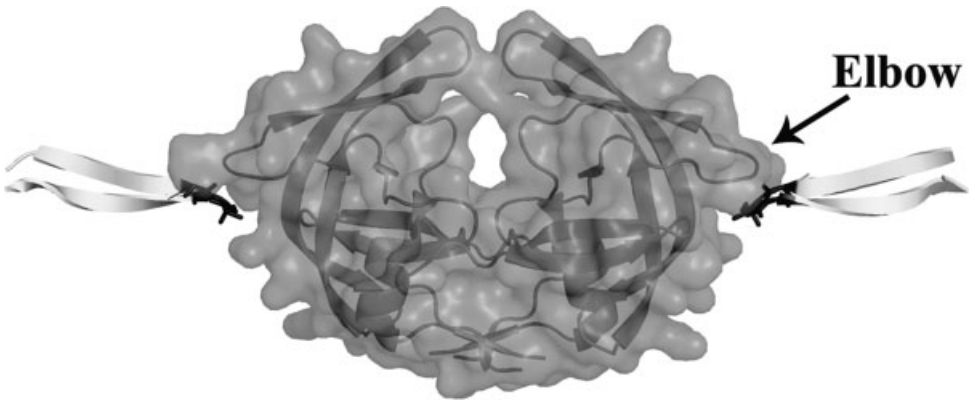

Figure 1

The 1TW7 structure of HIVp, showing crystal contacts between neighboring flap tips and the elbow. The flap-tip residues in direct contact with the elbow cleft (residues 49–52) are shown in black.

cell and the elbow region of HIVp (Fig. 1). It has been proposed that this might be experimental corroboration of allosteric control. Recent Langevin dynamics (LD) simulations by Layten *et al.* showed that the conformation of HIVp seen in 1TW7 relaxes into the typical semi-open conformation in the absence of the crystal contacts.[8] When all packing neighbors within 15 Å of the central dimer were replicated and restrained to their location, the unrestrained central HIVp sampled only the more open conformation seen in 1TW7. Layten *et al.* definitively showed that the crystal contacts cause the deformation, but they were astute not to claim that those contacts proved or disproved allosteric modulation of the flaps.

The tips of the flaps are the regions that make contact with elbow residues in neighboring cells. The structure may be deformed through "pulling" the flap tips into the next cell, or they may be "pushed" through allosteric contact with the elbow. To provide evidence of allosteric control, altered dynamics of the flaps must be demonstrated when the contacts are made solely with the elbows. Furthermore, these contacts should be allowed full conformational freedom.

In this study, we truncated the points of contact to create small peptides associated to the elbow region of dimeric HIVp. The peptides failed to restrict the conformation of the flaps. When the peptides were restrained from dissociating from the elbow, the flaps still sampled the semi-open and open conformations. Even modifying the peptides to create more contact within the cleft failed to improve their control of the flaps. When unrestrained, all peptides quickly dissociated from the elbow in multiple simulations, showing that the contact seen in the 1TW7 crystal structure is simply opportunistic crystal packing, not allosteric control. Lastly, experimental testing of short model peptides failed to inhibit HIVp.

METHODS

Two small peptides were created based on the flap residues of HIVp in contact with the elbows in the 1TW7 structure. The first peptide consisted only of the residues in direct contact with the protease: Ac-Gly49-Ile50-Gly51-Gly52-NMe (GIGG). Figure 2(A) shows that the complementarity is relatively poor, and the contact skims the surface with no functional groups placed in the elbow cleft itself. Therefore, another tetrapeptide, Asp-D-Ile-D-Phe-Gly (DifG), was designed from the backbone of residues 49–52, using D-amino acids to better orient side chains directly into the cleft region and increase complementary contact [Fig. 2(B)]. The use of D-Ile and D-Phe was suggested by solvent-mapping aromatic and hydrophobic functional groups into the binding cleft of the protease elbow (data not shown).[15–18] The initial L-Asp was used to improve solubility and facilitate subsequent experimental testing of the model peptide.

The two GIGG tetrapeptides occupy a total of 1087 Å^2 of the solvent accessible surface area (SASA) of HIVp, and the DifG peptides occupy 1283 Å^2. Changing the chirality of the isoleucine increased the contact of each peptide by ~22 Å^2, and adding the phenylalanine side chain in the D-orientation added ~77 Å^2 of contact, resulting in each DifG peptide having almost 100 Å^2 of increased contact with the elbow cleft of HIVp. SASA was measured in NACCESS2.1.[19]

Both implicit and explicit solvent simulations were performed. A total of 16 simulations were carried out.

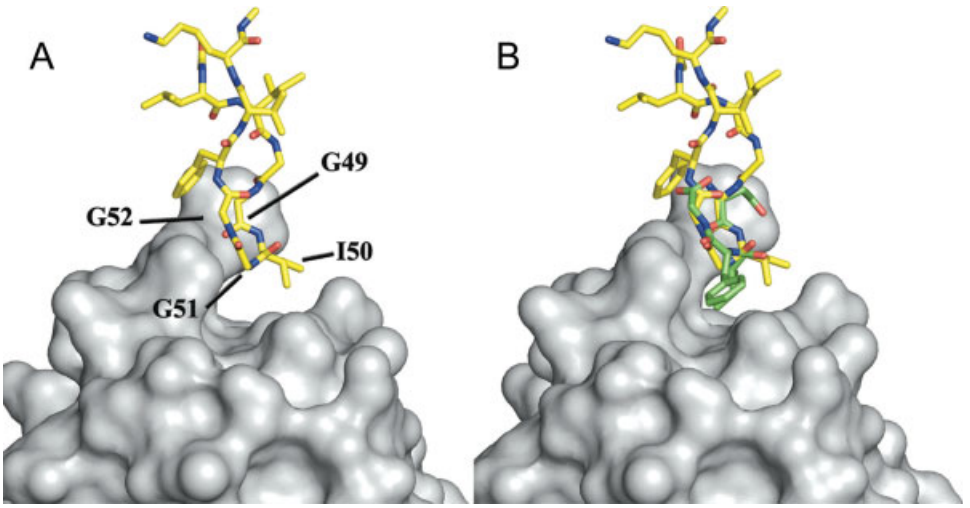

Figure 2

(**A**) The GIGG sequence makes no contacts into the base of the elbow cleft, but (**B**) using D-Ile50 and D-Phe51 (green) increases the peptide's contact with the sides and bottom of the cleft by ~100 Å^2.

Twelve independent LD simulations were run, six for each tetrapeptide starting from different random-number seeds. Two simulations of GIGG restrained in the elbow cleft were run, one implicit-solvent LD and one explicit-solvent MD. Two simulations of apo HIVp, LD and MD, were used as a control; the simulations were unrestrained and started from the conformation seen in 1TW7. Each simulation with GIGG or DifG had two peptide ligands, one in each elbow. This provided simulations of 12 DifG-HIVp associations (the six unrestrained LD) and 16 GIGG-HIVp associations (six unrestrained LD, one restrained LD, and one restrained MD) for analysis. Figure 3 shows the individual restraints applied for the simulations of GIGG restrained in the elbow. In the restrained simulations, an upper bound of 32 kcal/(mol · Å^2) and a lower bound of 0 kcal/(mol · Å^2) were used (weight was increased from 0.1 to 1 during the first phase of equilibration and then held constant at 1 for the extent of the simulation). This use of restraints kept the peptides associated to the elbow region but still allowed some flexibility for the peptides. It was desirable for the peptides, but not the artificial restraints, to control the conformational sampling of HIVp.

The implicit-solvent simulations used the LD protocol of Simmerling and coworkers,[8,20,21] while explicit-solvent protocol was based upon the work by Meagher and Carlson.[22] All simulations were based on the 1TW7 crystal structure of apo HIVp. PyMol[23] was used to propagate the unit cells and obtain the two protein chains in contact with the elbow region. Truncation of those chains into peptides was performed in MOE2006.08[24]; the modification of side chains for the peptide ligands was also done in MOE. Hydrogens were built using the tLEaP module in AMBER8,[25,26] and the FF99SB force field[27] was used. The time step was 1 fs and bonds to hydrogens were constrained. Temperature was controlled through

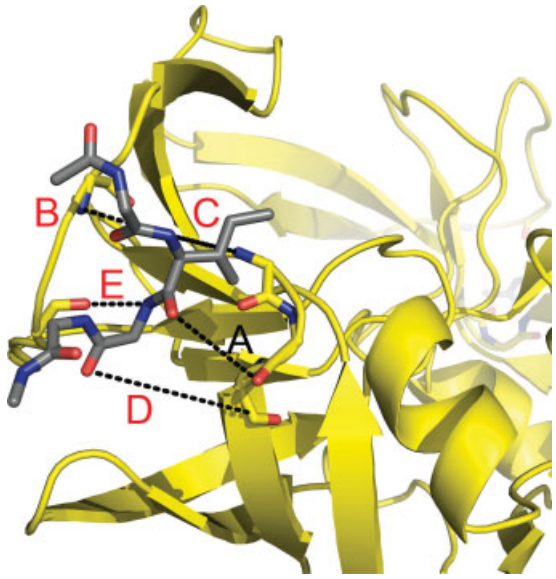

Figure 3

Distance restraints employed in the LD and MD simulations of the GIGG-HIVp complex. The Ac-G1-I2-G3-G4-NMe ligand was held in the elbow cleft with restraints woven between the elbow and the cantilever regions: (**A**) I2(O) – Q61(O) = 6.17 Å, (**B**) I2(N) – R41(N) = 4.83 Å, (**C**) I2(N) – D60(N) = 7.55 Å, (**D**) G3(O) – V62(O) = 10.42 Å, (**E**) G3(N) – P39(O) = 4.08 Å. These values are upper limits of the allowed distances; there is no penalty for forming closer contacts. This prevents dissociation but allows for some freedom in sampling and adaptation outside the crystalline environment of 1TW7.

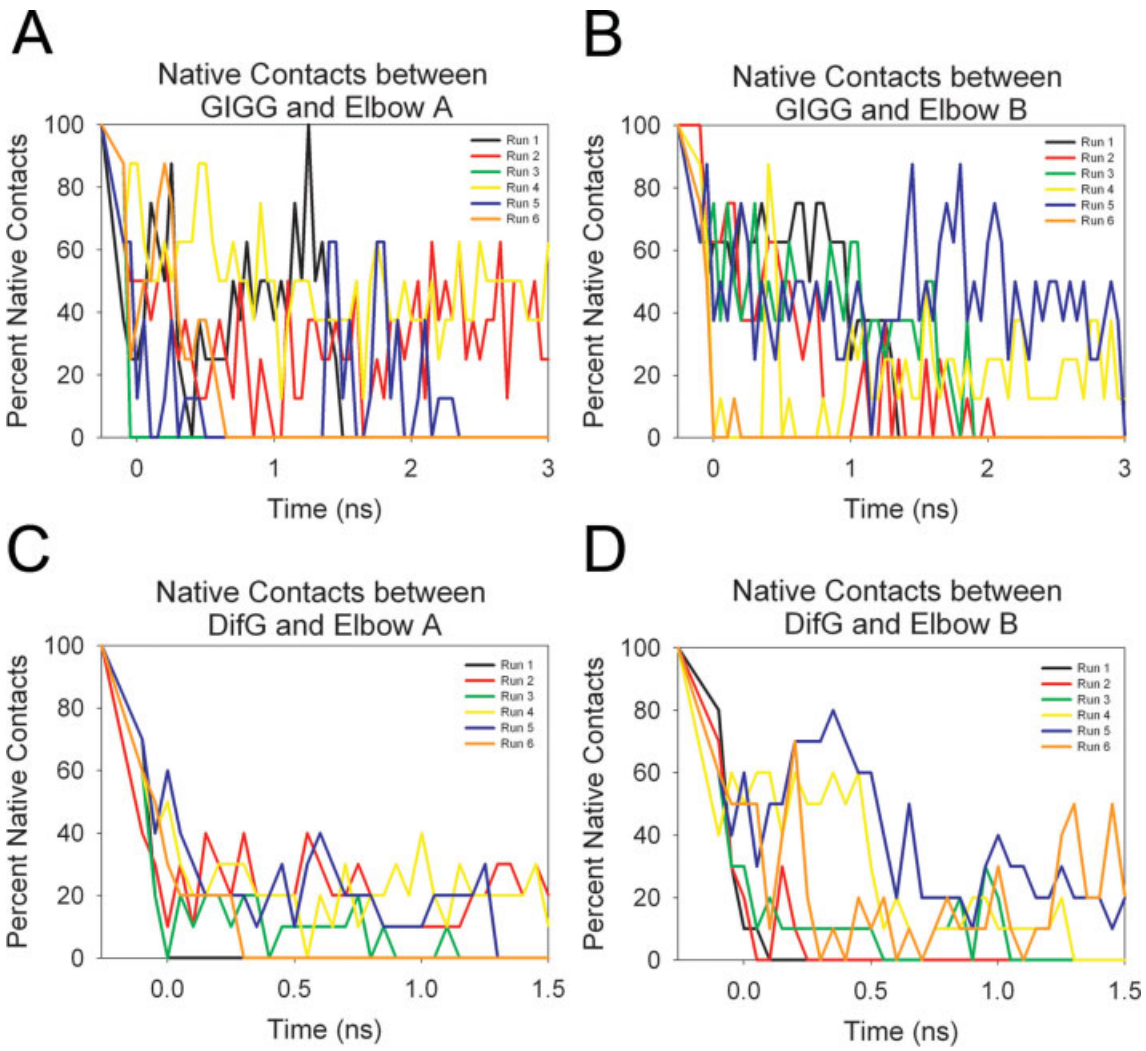

Figure 4

Percent of native contacts over the course of the unrestrained LD for (**A**, **B**) GIGG or (**C**, **D**) DifG bound to HIVp.

LD with a collision frequency of 1 ps^{-1}. A modified generalized born solvation model[28] was implemented to represent aqueous solvation in the LD simulations.

The explicit-solvent MD protocol was similar to the implicit setup. TIP3P waters were used to solvate the system as an octagonal box (14,190 waters in the GIGG-HIVp complex and 10,492 waters around the apo HIVp from 1TW7). Chloride ions were added to neutralize, and the Particle Mesh Ewald method was used to calculate long-range electrostatic interactions. A cutoff of 10 Å for nonbonded vdW interactions was employed.

Equilibration was accomplished over a series of six phases. The system was gradually heated from 100 to 300 K over the first two steps and remained at 300 K thereafter. Restraints were placed on all heavy atoms and gradually removed over the first four phases using force constants from 2.0 to 0.1 kcal/(mol · $Å^2$). In the fifth phase, only the backbone atoms were restrained with a force constant of 0.1 kcal/(mol · $Å^2$). Phases 1 through 3 were each 10 ps; phases 4 and 5 were 50 ps. In the last phase of equilibration, all atomic force restraints were removed, and the system sampled for 200 ps at 300 K. For the unrestrained simulations, the subsequent production phase was performed under the same conditions, sampling 1.5 ns for unrestrained DifG and 3 ns for unrestrained GIGG simulations. For the restrained LD and MD simulations of GIGG and the LD and MD simulations of apo HIVp from 1TW7, setup and equilibration was performed as before, except that the final temperature was 310 K. These systems were equilibrated during phase 6 for 2 ns and the production run lasted for 16 ns.

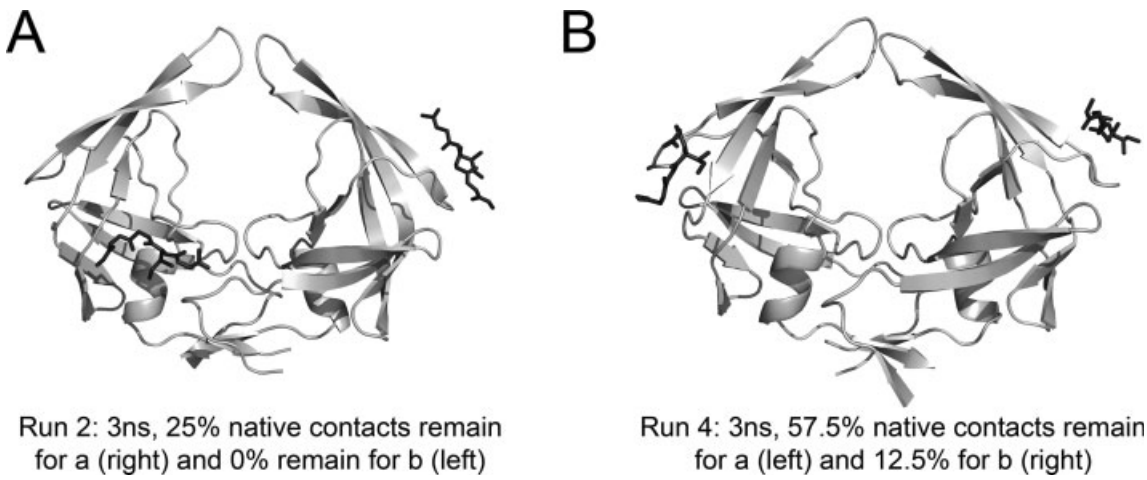

Figure 5

The 3-ns snapshot of runs 2 (**A**) and 4 (**B**) from the unrestrained LD simulations of the GIGG-HIVp complex. These images demonstrate that while some of the native contacts are retained, the tetrapeptide is no longer associating with the elbow pocket (compare with contacts in Fig. 1).

Snapshots were taken every 1 ps for analysis in the ptraj module of AmberTools 1.0.[29,30] For each snapshot, the rmsd to the 1TW7 conformation was calculated for the Cα core of the protease (all residues except 43–58 and 43′–58′). The rmsd of flap Cα atoms was measured from the core-overlaid frame of reference. Snapshots from the simulation were also manually viewed to confirm that the peptides were dissociating and not simply finding an alternative binding mode. The percentage of native contacts between HIVp and the tetrapeptides were calculated over the course of the unrestrained LD, using the MMTSB code.[31] The root-mean-squared fluctuation (rmsf) of the backbone heavy atoms was calculated in ptraj for each residue.

A FRET-based assay was used to determine the inhibition constants of GIGG and DifG against HIVp.[16,32,33] The substrate in the assay was a labeled oligopeptide, RE(EDANS)SQNYPIVQK(DABCYL)R, purchased from Molecular Probes (Cat. No. H-2930); recombinant HIVp was purchased from BaChem Biosciences (Cat. No. H-9040.0100), and the tetrapeptides GIGG and DifG were synthesized by the Peptide Core at the University of Michigan Medical School. Pepstatin A (PepA) was used as a positive control for inhibition of HIVp (USB, lot no. 110018). The fluorimetric assays were performed in triplicate in 384-well plates (Corning No. 3676) and read using a SpectraMax M5 (Molecular Devices). Protease cleavage of the substrate releases EDANS from DABCYL, and EDANS fluorescence was monitored with excitation/emission wavelengths of 340/490 nm with a cutoff filter at 475 nm.

To help prevent peptide and protease precipitation, PEG-400 was diluted in buffer A (20 m*M* phosphate, 1 m*M* DTT, 1 m*M* EDTA, 20% glycerol, and 0.1% CHAPS at pH 5.1); 1 μL was added to each well (PEG-400 final concentration, 0.1%). Two microliters of compound was diluted in water and then added to the wells to provide final concentrations ranging 50–250 μ*M*, followed by dilution of 5 μL HIVp in buffer A (final concentration of 30 n*M*). The peptide and protease were incubated for 45 min at room temperature; then, 12 μL of substrate (diluted in buffer A to a final concentration of 2 μ*M*) was added to initiate the assay.

RESULTS AND DISCUSSION

Unrestrained LD simulations of peptide-HIVp complexes

Twelve independent, LD simulations of HIVp with peptide ligands were initiated from the 1TW7 crystal structure (six for GIGG and six for DifG). The tetrapeptides were unrestrained and allowed to freely associate with the protease. Throughout the first five steps of equilibration, the peptides remained in contact with the structure, with a maximum rmsd of 2.5 Å to their initial location based on 1TW7. However, all of the peptides dissociated from the protease during the production phase of the simulations. HIVp itself remained stable, with flap tips sampling freely. Figure 4 shows the percentage of native contacts lost over the simulation for unrestrained GIGG and DifG peptides. Although runs 2 and 4 of the GIGG-HIVp complex still retain some of the native contacts at 3 ns, Figure 5 demonstrates that the peptides are no longer positioned in the protease elbow. None of the unrestrained tetrapeptides remained in the binding cleft throughout the simulation. The addi-

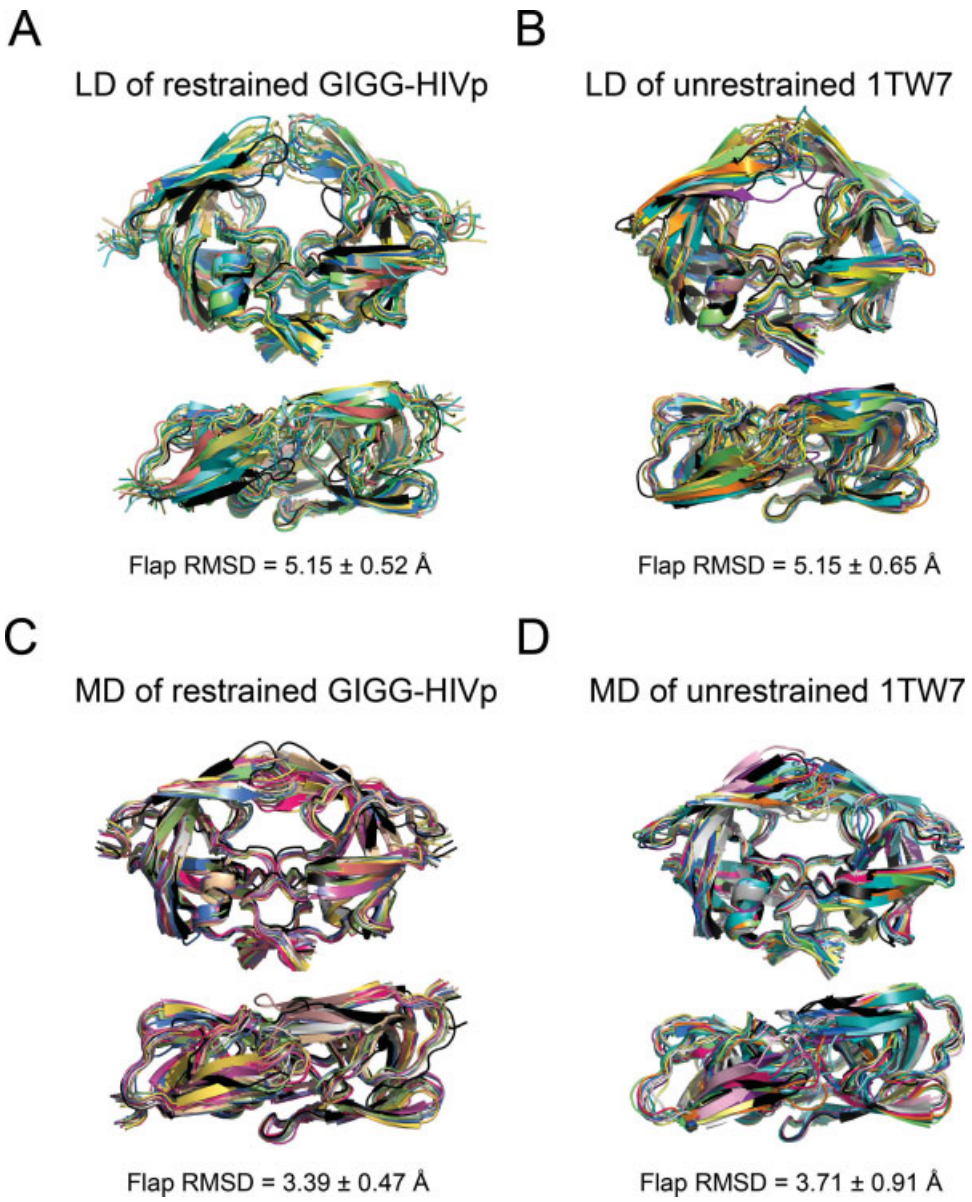

Figure 6

Representative cluster families display the conformations sampled in 85% of each simulation. Each set is overlaid to the crystal structure conformation of 1TW7 (in black): (**A**) LD of the restrained GIGG-HIVp, (**B**) LD of unrestrained apo HIVp, (**C**) MD of restrained GIGG-HIVp, and (**D**) MD of unrestrained apo HIVp. The structures are overlaid by the Cα of the core residues (all residues except the flaps 43–58 and 43′–58′), and the RMSD of the flap region is noted.

tional contacts provided by the DifG modifications showed no improvement.

LD and MD of restrained GIGG-HIVp compared with unrestrained HIVp, both based on 1TW7

There are many reasons a ligand can be unstable in a simulation, so it was important to establish if conformational control of the flaps is possible if the peptides in contact with the elbows in 1TW7 cannot dissociate. As outlined in the "Methods" section, we restrained GIGG to remain at the elbow for both the explicit- and implicit-solvent simulations of 16 ns. As a "control," two 16-ns simulations of apo HIVp (based on 1TW7 without ligands or restraints) were performed and analyzed in comparison to the complex. The LD simulations were performed to access greater sampling of conformational

states, while the MD were generated to more accurately sample the motion of the system in explicit solvent.

Over the course of the production sampling, all trajectories demonstrated stability of the core HIVp residues. However, both the free and bound systems demonstrated considerable motion in the flap region. In these simulations, the flaps move away from their wide-open position in the crystal structure of 1TW7 and sample the semi-open conformations. In fact, the apo handedness of the semi-open state is obtained with both the restrained and free LD simulations (the wide-open flaps have the handedness of the bound state). Sampling is reduced in the explicit-solvent simulation, and neither the restrained nor unrestrained simulation changed flap handedness.

To quantify the sampling, snapshots from every 1 ps of the 16-ns simulation were grouped into 20 distinct conformational clusters, using the means algorithm within ptraj.[29] Analyzing the conformational behavior of the families focused on the flexible flaps (details of the core, flap, and global comparisons of rmsd across all families are given in the Supplemental Information). The core of the protein was very stable and similar across all of the simulations, but the flaps were quite mobile. The core (all residues except the flaps) of each conformation was overlaid to the 1TW7 conformation via rmsd-fit of the Cα. The flexibility across families was then measured as the Cα-rmsd (measurement, not an additional overlay) for the flap residues 43–58 and 43′–58′. For both the LD and MD simulations, the conformations from the restrained GIGG-HIVp complex showed nearly identical sampling as those from the unrestrained apo HIVp. The rmsd of the Cα of the flaps are 5.26 ± 0.56 Å and 5.32 ± 0.66 Å for the LD of the restrained GIGG-HIVp complex and the unrestrained apo HIVp, respectively. For the MD, the rmsd of the flaps are 3.17 ± 0.60 Å and 3.61 ± 0.74 Å for the restrained and unrestrained simulations, respectively. Though the restrained simulations show slightly less sampling, it is insignificant, especially when compared with the range of rmsd across the 20 conformational families. We also analyzed these simulations while focusing on only the most densely populated states and excluding the rare conformations which have less statistical significance. The conformational families with the most occupants were chosen; the largest families that represented ~85% of each trajectory were used (11 conformational families from the MD and LD of the restrained complex; 12 from the unrestrained LD and MD). Figure 6 shows the large conformational sampling across 85% of the LD and MD (note that the rmsd values are slightly different than those aforementioned which reflect the variation across all 20 conformational families from the simulations).

To provide further quantitative assessment of the conformational sampling, Figure 7 provides rmsd analyses over the time course of the LD simulations. There is little difference in flap mobility between the unrestrained HIVp and the GIGG-bound complex, with both freely sampling flap conformations between 3 and 11 Å rmsd of the placement in the 1TW7 structure. One of the standard metrics for assessing the conformational state of the flaps is the distance between Asp25 and Ile50. In 1TW7, the skewed-open structure has a distance of 18.8 Å. In the semi-open structure 1HHP, this distance is 17.2 Å, while a typical closed structure 1PRO has a distance of 14.1 Å. As can be seen in Figure 8, the flaps in both the restrained and unrestrained LD simulations sample semi-open and open structures. The same analysis for the MD simulations is provided in the Supplemental Information. The explicit solvation reduces the degree of sampling (seen in Fig. 7) and biases more semi-open and closed conformations. However, the restrained and unrestrained simulations are not significantly different in their conformational sampling.

Experimental testing of peptides

To further support our conclusions, we conducted experimental inhibition assays. A fluorimetric assay was used to discern the inhibitory potency of the GIGG and DifG peptides. Consistent with the simulations, we found no inhibition of HIVp by either tetrapeptide at concentrations of 250 μ*M* (Fig. 9).

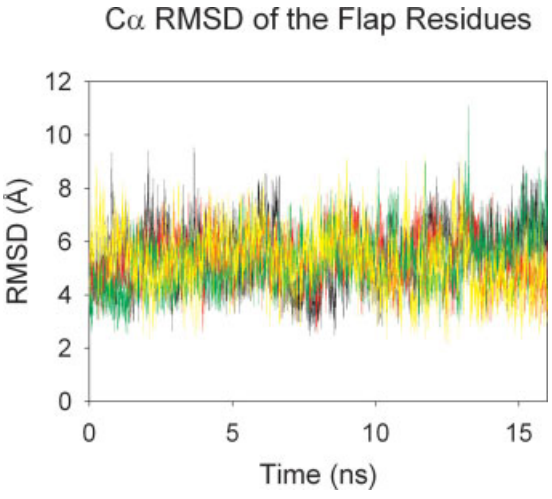

Figure 7

A wide degree of conformational sampling is seen in the LD simulations, whether GIGG is present or not. Both flaps of the restrained GIGG-HIVp (yellow and green lines) and unrestrained apo HIVp (red and black lines) simulations are shown. The snapshots were overlaid with respect to the Cα atoms of the core of the dimer in 1TW7, and the RMSD of only the flap Cα (residues 43–58 and 43′–58′) are shown above.

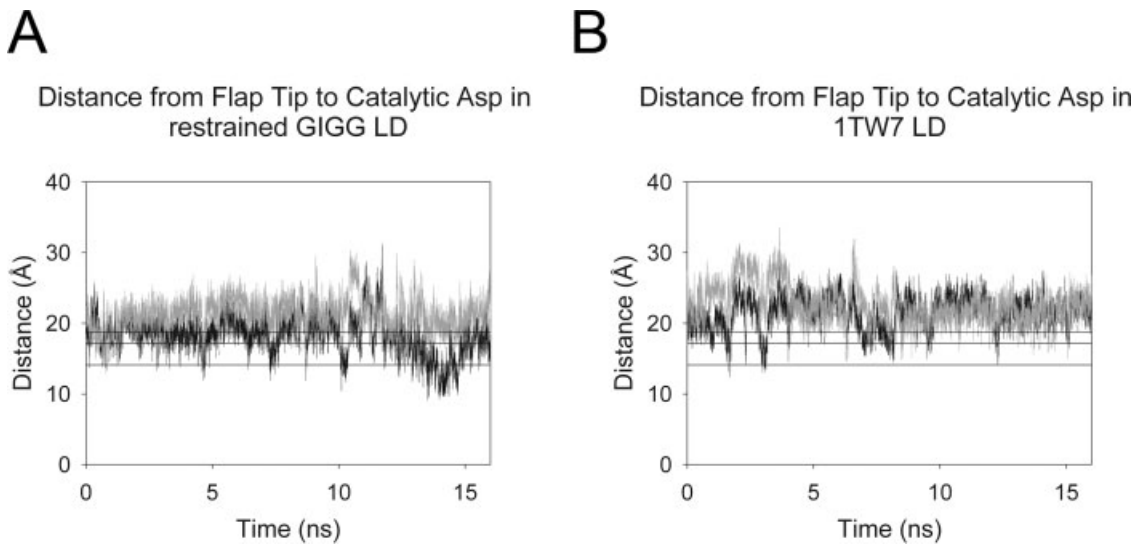

Figure 8

The distance from the flap tips Ile50/50′ to the catalytic Asp25/25′ during the implicit-solvent LD of (**A**) the restrained, GIGG-HIVp complex and (**B**) the unrestrained, apo HIVp. The individual flaps have different colors in each plot. Horizontal, black lines denote the distances seen in different conformational states: the skewed-open 1TW7 is 18.8 Å, the semi-open 1HHP is 17.2 Å, and the closed 1PRO is 14.1 Å.

CONCLUSIONS

As demonstrated by both unrestrained and restrained simulations of protease–ligand complexes, the contacts seen in the 1TW7 crystal structure do not exemplify allosteric control. The peptide-HIVp complexes were unstable and freely dissociated. The interactions appear too weak, even when modified to improve the contacts. Despite restraints to maintain contacts to the elbow region, their association with HIVp had no significant affect on flap mobility. Perryman *et al.* have used restraints within the elbow region to control flap dynamics,[9] but it appears that maintaining only the elbow contacts in 1TW7 is not able to force this control. Furthermore, experimental testing showed no inhibitory activity by small peptides representing those crystal contacts. This study further refines the conclusions of Layten *et al.*[8] to show that the altered conformation in 1TW7 is solely the result of packing effects and not the result of a symmetric environment which fortuitously presents allosteric contacts.

We emphasize that this study does not refute the possibility of allosteric control via the elbow region, but it does indicate that peptide-based molecules may be less appropriate for these efforts. Hornak *et al.* showed that it was possible for the small inhibitor XK263 to correct itself during LD sampling after initial improper placement.[20] This result does not mean that all ligands can correct poor contacts during an LD simulation, but we may have expected at least one of 12 peptides to correct their placement into a stable alternative location if peptide ligands were appropriate. Our results could explain why no allosteric inhibitors have been found serendipitously, despite a significant effort to develop competitive inhibitors using peptide scaffolds.[34]

It is possible that effective allosteric inhibitors will require more contacts between the structural features of HIVp. The contacts in 1TW7 place the flap tip in contact

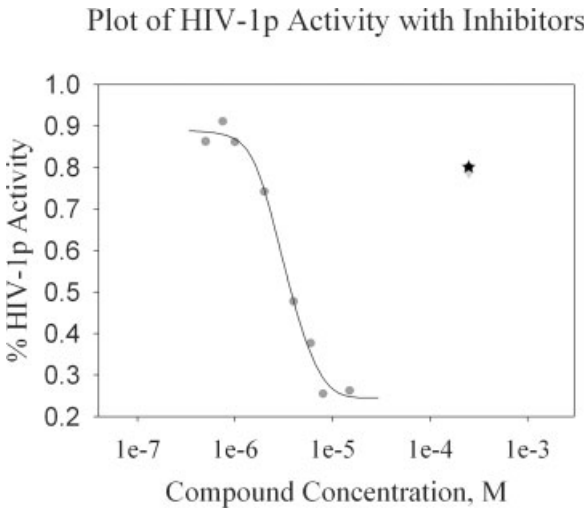

Figure 9

The activity of HIVp in the presence of 250 μM peptides is given: DifG (black star) and the model peptide for GIGG (Ac-GIGGK, light gray triangle). The IC_{50} curve of the control PepA is also shown (gray circles).

with only the elbow and cantilever (residues 59–75) regions. As such, these were the only contacts maintained in our simulations. However, the nearby "fulcrum" region (residues 11–22) has also been shown to be correlated with flap motion.[6,13,35,36] It is possible that a small molecule will have to contact all three regions to gain adequate allosteric control of a region as large as the flaps.

REFERENCES

1. Hornak V, Simmerling C. Targeting structural flexibility in HIV-1 protease inhibitor binding. Drug Discov Today 2007;12:132–138.
2. Toth G, Borics A. Closing of the flaps of HIV-1 protease induced by substrate binding: a model of a flap closing mechanism in retroviral aspartic proteases. Biochemistry 2006;45:6606–6614.
3. Toth G, Borics A. Flap opening mechanism of HIV-1 protease. J Mol Graph Model 2006;24:465–474.
4. Ding F, Layten M, Simmerling C. Solution structure of HIV-1 protease flaps probed by comparison of molecular dynamics simulation ensembles and EPR experiments. J Am Chem Soc 2008;130:7184–7185.
5. Chang CE, Trylska J, Tozzini V, McCammon JA. Binding pathways of ligands to HIV-1 protease: coarse-grained and atomistic simulations. Chem Biol Drug Des 2007;69:5–13.
6. Trylska J, Tozzini V, Chang CE, McCammon JA. HIV-1 protease substrate binding and product release pathways explored with coarse-grained molecular dynamics. Biophys J 2007;92:4179–4187.
7. Rick SW, Erickson JW, Burt SK. Reaction path and free energy calculations of the transition between alternate conformations of HIV-1 protease. Proteins 1998;32:7–16.
8. Layten M, Hornak V, Simmerling C. The open structure of a multidrug-resistant HIV-1 protease is stabilized by crystal packing contacts. J Am Chem Soc 2006;128:13360–13361.
9. Perryman AL, Lin JH, McCammon JA. HIV-1 protease molecular dynamics of a wild-type and of the V82F/I84V mutant: possible contributions to drug resistance and a potential new target site for drugs. Protein Sci 2004;13:1108–1123.
10. Piana S, Carloni P, Rothlisberger U. Drug resistance in HIV-1 protease: flexibility-assisted mechanism of compensatory mutations. Protein Sci 2002;11:2393–2402.
11. Zoete V, Michielin O, Karplus M. Relation between sequence and structure of HIV-1 protease inhibitor complexes: a model system for the analysis of protein flexibility. J Mol Biol 2002;315:21–52.
12. Perryman AL, Lin JH, Andrew McCammon J. Optimization and computational evaluation of a series of potential active site inhibitors of the V82F/I84V drug-resistant mutant of HIV-1 protease: an application of the relaxed complex method of structure-based drug design. Chem Biol Drug Des 2006;67:336–345.
13. Perryman AL, Lin JH, McCammon JA. Restrained molecular dynamics simulations of HIV-1 protease: the first step in validating a new target for drug design. Biopolymers 2006;82:272–284.
14. Martin P, Vickrey JF, Proteasa G, Jimenez YL, Wawrzak Z, Winters MA, Merigan TC, Kovari LC. "Wide-open" 1.3 Å structure of a multidrug-resistant HIV-1 protease as a drug target. Structure 2005;13:1887–1895.
15. Bowman AL, Lerner MG, Carlson HA. Protein flexibility and species specificity in structure-based drug discovery: dihydrofolate reductase as a test system. J Am Chem Soc 2007;129:3634–3640.
16. Damm KL, Ung PM, Quintero JJ, Gestwicki JE, Carlson HA. A poke in the eye: inhibiting HIV-1 protease through its flap-recognition pocket. Biopolymers 2008;89:643–652.
17. Meagher KL, Carlson HA. Incorporating protein flexibility in structure-based drug discovery: using HIV-1 protease as a test case. J Am Chem Soc 2004;126:13276–13281.
18. Meagher KL, Lerner MG, Carlson HA. Refining the multiple protein structure pharmacophore method: consistency across three independent HIV-1 protease models. J Med Chem 2006;49:3478–3484.
19. Hubbard SJ, Thornton JM. Naccess 2.1.1., University of Manchester, Manchester, UK, 1993.
20. Hornak V, Okur A, Rizzo RC, Simmerling C. HIV-1 protease flaps spontaneously close to the correct structure in simulations following manual placement of an inhibitor into the open state. J Am Chem Soc 2006;128:2812–2813.
21. Hornak V, Okur A, Rizzo RC, Simmerling C. HIV-1 protease flaps spontaneously open and reclose in molecular dynamics simulations. Proc Natl Acad Sci USA 2006;103:915–920.
22. Meagher KL, Carlson HA. Solvation influences flap collapse in HIV-1 protease. Proteins: Struct Funct Genet 2005;58:119–125.
23. DeLano WL. The pymol molecular graphics system [MacPyMOL], DeLano Scientific, San Carlos, CA, 2002.
24. MOE 2005.06 (Molecular Operating Environment), Chemical Computing Group, Montreal, Canada, 2005.
25. Case DA, Cheatham TE, III, Darden T, Gohlke H, Luo R, Merz KM, Jr, Onufriev A, Simmerling C, Wang B, Woods RJ. The AMBER biomolecular simulation programs. J Comput Chem 2005; 26:1668–1688.
26. Case DA, Darden TA, Cheatham TE, III, Simmerling CL, Wang J, Duke RE, Luo R, Merz KM, Wang B, Pearlman DA, Crowley M, Brozell S, Tsui V, Gohlke H, Mongan J, Hornak V, Cui G, Beroza P, Schafmeister C, Caldwell J, Ross W, Kollman P. Amber 8, University of California, San Francisco, CA, 2004.
27. Hornak V, Abel R, Okur A, Strockbine B, Roitberg A, Simmerling C. Comparison of multiple AMBER force fields and development of improved protein backbone parameters. Proteins: Struct Funct Genet 2006;65:712–725.
28. Onufriev A, Bashford D, Case DA. Modification of the generalized born model suitable for macromolecules. J Phys Chem B 2000; 104:3712–3720.
29. Shao J, Tanner SW, Thompson N, Cheatham TE. Clustering molecular dynamics trajectories. I. Characterizing the performance of different clustering algorithms. J Chem Theory Comp 2007;3:2312–2334.
30. Case DA, Darden TA, Cheatham TE, I, Simmerling CL, Wang J, Duke RE, Luo R, Crowley M, Walker RC, Zhang W, Merz KM, Wang B, Hayik S, Roitberg A, Seabra G, Kolossváry I, Wong KF, Paesani F, Vanicek J, Wu X, Brozell SR, Steinbrecher T, Gohlke H, Yang L, Tan C, Mongan J, Hornak V, Cui G, Mathews DH, Seetin MG, Sagui C, Babin V, Kollman PA. Amber 10, University of California, San Francisco, CA, 2008.
31. Feig M, Karanicolas J, Brooks CL, III. Mmtsb tool set: enhanced sampling and multiscale modeling methods for applications in structural biology. J Mol Graph Model 2004;22:377–395.
32. Matayoshi ED, Wang GT, Krafft GA, Erickson J. Novel fluorogenic substrates for assaying retroviral proteases by resonance energy transfer. Science 1990;247:954–958.
33. Toth MV, Marshall GR. A simple, continuous fluorometric assay for HIV protease. Int J Pept Protein Res 1990;36:544–550.
34. Babine RE, Bender SL. Molecular recognition of protein-ligand complexes: applications to drug design. Chem Rev 1997;97:1359–1472.
35. Tozzini V, McCammon JA. A coarse grained model for the dynamics of flap opening in HIV-1 protease. Chem Phys Lett 2005;413: 123–128.
36. Tozzini V, Trylska J, Chang CE, McCammon JA. Flap opening dynamics in HIV-1 protease explored with a coarse-grained model. J Struct Biol 2007;157:606–615.